Detection of COVID-19, lung opacity, and viral pneumonia via X-ray using machine learning and deep learning

Hajar Lamouadene [a], Majid EL Kassaoui [a,e], Mourad El Yadari [b], Abdallah El Kenz [a], Abdelilah Benyoussef [a,c], Amine El Moutaouakil [d,*], Omar Mounkachi [a,e]

[a] Laboratory of Condensed Matter and Interdisciplinary Sciences, Physics Department, Faculty of Sciences, Mohammed V University in Rabat, Morocco
[b] ENSAM-R - Université Mohammed V de Rabat, Morocco
[c] Hassan II Academy of Science and Technology, Rabat, Morocco
[d] Department of Electrical and Communication Engineering, College of Engineering, UAE University, P.O. Box: 15551, Al Ain, United Arab Emirates
[e] College of computing, Mohammed VI Polytechnic University, Lot 660, Hay Moulay Rachid Ben Guerir, 43150, Morocco

ARTICLE INFO

ABSTRACT

The COVID-19 pandemic has significantly strained healthcare systems, highlighting the need for early diagnosis to isolate positive cases and prevent the spread. This study combines machine learning, deep learning, and transfer learning techniques to automatically diagnose COVID-19 and other pulmonary conditions from radiographic images. First, we used Convolutional Neural Networks (CNNs) and a Support Vector Machine (SVM) classifier on a dataset of 21,165 chest X-ray images. Our model achieved an accuracy of 86.18 %. This approach aids medical experts in rapidly and accurateky detecting lung diseases. Next, we applied transfer learning using ResNet18 combined with SVM on a dataset comprising normal, COVID-19, lung opacity, and viral pneumonia images. This model outperformed traditional methods, with classification rates of 98 % with Stochastic Gradient Descent (SGD), 97 % with Adam, 96 % with RMSProp, and 94 % with Adagrad optimizers. Additionally, we incorporated two additional transfer learning models, EfficientNet-CNN and Xception-CNN, which achieved classification accuracies of 99.20 % and 98.80 %, respectively. However, we observed limitations in dataset diversity and representativeness, which may affect model generalization. Future work will focus on implementing advanced data augmentation techniques and collaborations with medical experts to enhance model performance.This research demonstrates the potential of cutting-edge deep learning techniques to improve diagnostic accuracy and efficiency in medical imaging applications.

1. Introduction

The global outbreak of the coronavirus disease (COVID-19) in December 2019 has profoundly impacted public health, necessitating the development of rapid and accurate diagnostic methods. Early detection of COVID-19 is crucial for isolating positive cases and preventing the spread of the virus. Traditional diagnostic approaches, such as reverse transcription polymerase chain reaction (RT-PCR) suffer from delayed detection times and varying accuracy, while imaging techniques like X-rays and CT scans offer a faster and more detailed understanding of pulmonary conditions [1].

Artificial intelligence (AI), especially machine learning (ML) and deep learning (DL), has played an increasingly pivotal role in advancing medical diagnostics as well as in other scientific domains, notably in materials science [2–4]. Among these techniques, convolutional neural networks (CNNs) have demonstrated significant potential in processing medical images for disease detection [5]. Several studies have shown that CNN-based models can effectively diagnose COVID-19 from radiographic images, such as X-rays and CT scans [6]. However, despite these advances, the secure handling of medical data remains a critical concern, a challenge that can be addressed through federated learning, which allows model training on decentralized data without compromising patient privacy [7].

Despite the promise of CNN-based diagnostic tools, existing methods continue to face notable challenges, particularly regarding the ability to distinguish COVID-19 from other pulmonary conditions such as viral pneumonia. These challenges are often exacerbated by limited dataset diversity, slow inference times, and difficulties in distinguishing

---

between similar conditions [8]. Traditional deep learning models rely heavily on large volumes of labeled data and substantial computational resources, which can limit their applicability in certain healthcare environments. To address these issues, hybrid models combining deep feature extraction through CNNs and classification with traditional machine learning algorithms, such as support vector machines (SVMs) have been proposed [9]. Although these models show promise, they still face challenges related to generalization, hyperparameter tuning, and optimization constraints.

In this study, we propose a novel approach that integrates deep learning and transfer learning to enhance the accuracy and efficiency of automatic pulmonary condition detection from radiographic images. Specifically, we leverage ResNet18, a well-established deep CNN architecture known for its high performance in image classification tasks, and combine it with SVM for the classification of lung conditions [10]. By utilizing transfer learning, we aim to improve model performance, reduce training time, and address challenges associated with limited data availability [11]. Our approach enables more accurate differentiation between COVID-19, viral pneumonia, lung opacity, and healthy lungs, ultimately contributing to improved diagnostic outcomes. This study introduces a diagnostic framework that merges ResNet18-based deep feature extraction with SVM classification, demonstrating considerable accuracy improvements when employing transfer learning [12]. Furthermore, we address the challenge of data privacy by suggesting federated learning as a viable solution to mitigate privacy concerns in medical AI [13]. The remainder of this paper outlines our methodology, presents the experimental results, and discusses the broader implications of our findings. We conclude with suggestions for future work, including expanding dataset diversity through augmentation techniques and establishing collaborations with clinical experts to further improve the accuracy and applicability of automatic radiographic image detection in medical settings.

Our research aims to advance the detection and differentiation of COVID-19, viral pneumonia, and lung opacity from healthy lungs [14, 15]. This study underscores the potential of combining DL and ML techniques for designing accurate and computationally efficient diagnostic tools, contributing to improved healthcare outcomes for pulmonary diseases [16,17]. Notably, our approach aligns with the work presented in "Diagnosis of COVID-19 CT Scans Using Convolutional Neural Networks" (SN Computer Science, 5(5), 625), which demonstrates the efficacy of CNN-based models like ResNet152 and Dense-Net201 for diagnosing COVID-19 through CT scans. However, in contrast to that study, our method applies ResNet18 and SVM for enhanced accuracy, specifically tailored for radiographic images, which are more widely accessible in clinical settings. This study also explores hyperparameter tuning and implement techniques to address data imbalance, aspects that are critical for improving model reliability [18]. The following sections will outline our methodology, present our findings, discuss their implications, and propose future directions for enhancing automatic radiographic image detection in the medical field [19].

- Section (I) describes the dataset, pretreatment methods, models and statistical analysis conducted in this study. Additionally, we provide a detailed background of architectural adjustments on the CNN, ResNet 18, VGG, SVM and transfer learning between ResNet 18-SVM.
- Section (II) we present two sets of results. Firstly, a comprehensive benchmarking of the performance of various models for multi-class classification from chest X-ray (CXR) images. Secondly, we explore the testing conducted on the custom of transfer learning approach.
- Finally, Section (III) draws conclusions and discusses future work.

2. Methodology

Machine learning is primarily used through traditional approaches to detect and classify various anomalies. The main issue with this approach is the excessive computational burden and its limited performance. In this section, we provide a detailed description of the data, analysis techniques, as well as data collection and annotation, as shown in Fig. 1. We then discuss the training and design of CNN architectures and transfer learning.

2.1. COVID-19 X-ray database

The purpose of this approach is to detect and classify COVID-19, viral pneumonia, and lung opacity on the chest X-ray images similar to the samples shown in Fig. 2(a–d). The used set of X-ray data has been downloaded from the Kaggle database at https://www.kaggle.com/taws ifurrahman/covid19-radiography-database.

2.1.1. Data augmentation

In deep learning, it is often desirable to implement precise data augmentation to avoid overfitting issues. This can also be mitigated through a well-designed data growth strategy [20,21]. The latter can be developed to improve sample size, thus reducing the impact of imbalanced data. Data augmentation is a strategy that addresses the issue of imbalanced data by introducing slight variations to existing data [22, 23]. For example, Soumya Ranjan Nayak et al. augmented the training of X-ray images by rotating them clockwise by 5°, scaling them by 15 %, flipping the images horizontally, and adding Gaussian noise with a mean of 0 and a variance of 0.25 [24] as shown in Fig. 3 (a).

These methods do not generate new visual features in the images that could enhance the overall learning capabilities of the algorithm used and the network's generalization capabilities. Similarly, color, texture, and geometry-based augmentation techniques are not as popular due to their various drawbacks. Although a wide variety of other interesting methods have been developed in the past, only geometric transformations are currently commonly used. In this study, we used image rotation for geometric transformation to augment the chest X-ray images. While this technique allows for data diversification and improves classification, it also has drawbacks, such as additional memory, conversion, and computational costs, as well as extra learning time [25]. The rotation augmentations have been applied to images belonging to the four classes shown in Table 1, which contain a smaller amount of data.

2.1.2. CNN architecture

In this work, CNN, which is a cutting-edge sphere of machine learning inspired by the human brain, was used to classify images into COVID-19, normal, viral pneumonia and lung opacity. Fig. 3 (b) summarizes the steps of the CNN architecture for the differentiation of the different classes. Here, the CNN functions similarly to a human visual system, making it well-suited for two-dimensional images. This approach is particularly effective for medical image analysis, as demonstrated by Dhiman et al. [26], who achieved a classification accuracy of 98.54 % for COVID-19 detection using ResNet101 and the J48 algorithm. Thus, CNN analyzes images with pixel patterns to extract feature maps. However, the units are related to the previous layers from the core weights which are modified during formation through a process of backpropagation. Since all units use similar kernels, less weight is generated per convolutional layer. Indeed, the flats produced with CNN to achieve the objective of classifying the thoracic image are as following equation:

$$f(x) = \max(0, x) \tag{1}$$

Where, f(x) is the activation function to make the data on a linear unit in range 0, x. The pooling eliminated some important elements, thus leading to overlapped pooling 3*3. In conventional layers, as per eq. (2) functionality, the cards were padded with convolution. The use of padding ensured function cards of the same dimensions. Fig. 4 (a)
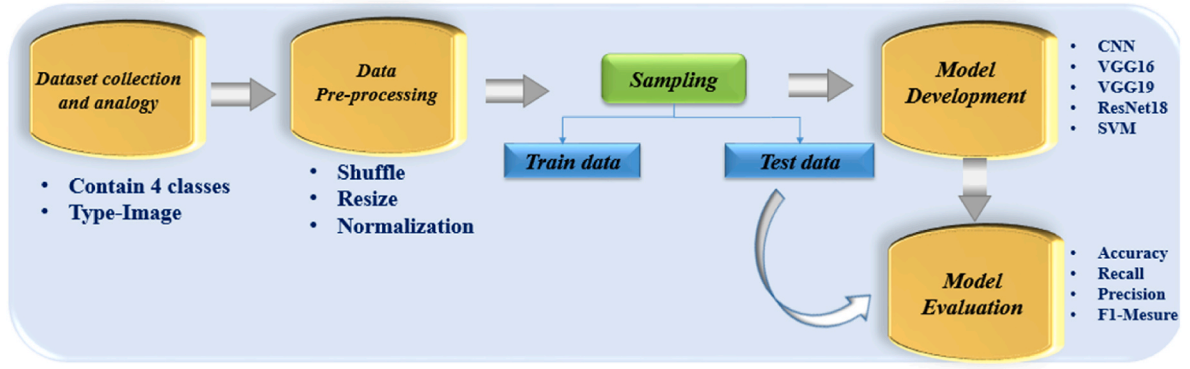
Fig. 1. The overall model of the proposed detection system.

(a) Normal   (b) Covid   (c) Lung-Opacity   (d) Viral Pneumonia
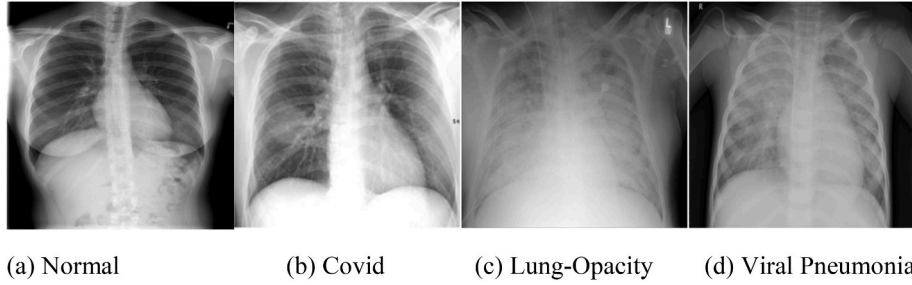
Fig. 2. Sample images from the Kaggle radiographic database.

represents the hyper-parameters as well as the values to classify the four classes COVID-19, normal, viral pneumonia and lung opacity. CNN was developed through python.

$$S\,(I,j) = (I^*K)(I,j) = \sum_{m}\sum_{n}I(m,n)K(i-m,j-n) \qquad (2)$$

In the following approach, the majority is formed by the vector of the handmade functionality that is determined as the input of the CNN network instead of the direct images. The image pixels, as well as the vectors of correlated characteristics, bind mainly and globally. Thus, we adopt a merged set of features as CNN network input [27].

These are the characteristic vectors with a length of 1024 that help to reduce the complexity of the formation of the CNN, which is also significant with an additional reduction in size. Similarly, this approach adopts a one-dimensional CNN network combining three layers of convolutions, one layer of pooling, one layer of abundant, and five layers fully connected. However, it is the PyTorch stream library (Tensor) that is optimized for the CNN model [5]. In the feature map representation, one uses a max pooling layer with a specified pooling size to reduce dimensionality and retain essential features.

As mentioned before, the network has four fully connected classification layers. The overfitting in the proposed CNN network is solved via the Softmax function and dropout layers. The output of the one-dimensional proposed CNN method follows equation (3):

$$O_k^l = f\left(C_k^l + \sum_{i=1}^{N_1-1} Conv\,1D\,\left(X_{ik}^{l-1}, t_i^{l-1}\right)\right) \qquad (3)$$

Where, C_k^l, X_{ik}^{l-1} and "f()" are the scalar bias of the kth neuron at the first layer, kernel weight from the ith neuron at layer l-1 to kth neurons at layer l, and the activation function, respectively. The CNN architecture aligns with state-of-the-art methods, such as in the work of [26], which highlights the importance of feature selection and optimization in achieving high performance in image classification tasks.

2.1.3. Deep learning: visual geometry group (VGG) model

Since 2014, the VGG model has been used for the classification of images. It consists of many convolutive layers activated by rectified linear unit (ReLU), and the kernel size of these convolutive VGG layers is specified in 3*3. There are also three different types of VGG models that have a similar structure and consist of successive layers of convolution and reassembly, followed by three fully connected layers. They differ only in the number of convolutional layers (11, 16 or 19) from which their name comes (VGG-11, VGG-16 and VGG-19). In this work, we used VGG-16 and VGG-19 for the classification of images in COVID-19, normal, viral pneumonia and lung opacity. The VGG-16 model had an accuracy of 75 % and VGG-19 had an accuracy of 77 %.

2.1.4. Deep learning: ResNet model

Residual neural network (ResNet) is a highly applied and preferred deep learning technique (DL) for the identification of COVID-19 X-ray images. The advantage of the ResNet model compared to other architectural models is that its performance does not degrade as the network depth increases. He et al. [28] showed that the ResNet model performs better in image classification than other DL architectures, indicating that it effectively extracts image features. On the other hand, the difference between ResNet-18, ResNet-34 and ResNet-50 lies in their block structures: the difference between ResNet-18 and ResNet-34 is in the number of repeated blocks, while the distinction between ResNet-34 and ResNet-50 lies in the internal composition of these blocks. In our approach, the ResNet-18 model was used to detect and classify Covid-19, normal, viral pneumonia and lung opacity. Additionally, an automated X-ray image analysis tool based on ResNet-18 was developed. The results showed an accuracy of 86 %.

2.1.5. Machine learning: SVM model

Support Vector Machine (SVM), as shown in Fig. 4 (b), allows the computer to learn how to perform classification and regression tasks, using an algorithm based on statistical learning and optimization theory, which increases the accuracy of predictions and completely avoids the
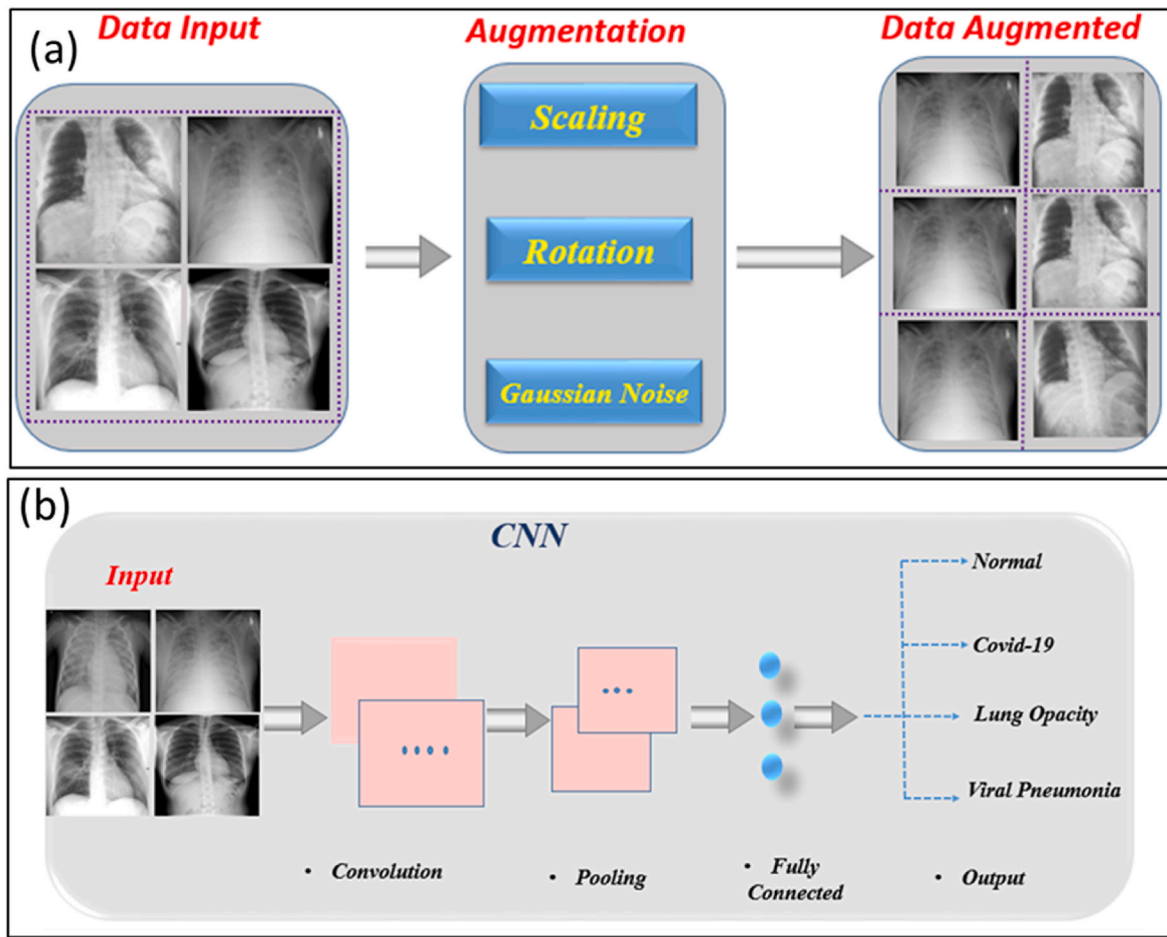
Fig. 3. (a) Sample results of data augmentation, (b) A basic CNN architecture for the multi-classification of COVID-19, Normal, Viral pneumonia and Lung Opacity.

Table 1
The number of samples belonging to each category in the COVID-19 radiographic database.

Category	Number of images
COVID-19	3616
Viral Pneumonia	1345
Normal	10192
Lung Opacity	6012
Total	21165

disadvantages of over-modification [29,30]. However, classifiers utilize a geometric representation of the data, where data points are plotted based on their characteristics or variables that influence classifications [31]. The role of the SVM is to define a decision boundary (linear decision area) that separates datasets with the largest deviation (maximum margin) on each side according to the optimization technique that can be solved using quadratic programming [32]. In this study, we used one of the most widely known kernel functions, the Gaussian kernel (also known as the Radial Base Function (RBF)) to enhance classification performance [33].

2.2. Transfer learning

Transfer learning, also known as learning transfer, is a machine learning approach where knowledge and models learned from a specific task are transferred and used to improve performance on another similar task. Rather than building a model from scratch for each task, transfer learning capitalizes on the information and representations learned during the pre-training on a related task [34].

Fig. 5 presents the main idea behind transfer learning; the characteristics and representations learned by a model on a general task can be useful for solving related specific tasks. For example, a pre-driven deep learning model on a large set of general image data, such as natural images, may have learned general visual features that can be reused for specific tasks, such as the classification of medical images.

In the context of transfer learning, there are generally two main approaches; Feature Extraction where the layers of a pre-driven model are used to extract the characteristics of the input data. These extracted features are then used as inputs for a new model or a task-specific machine learning algorithm [35]. Fine-tuning (Refining) refers to the process of adjusting the weights and parameters of a pre-trained model to adapt it to a new, task-specific dataset, thereby enhancing its performance for the given application. The first layers of the model can be frozen or kept as is, while the upper layers are adjusted to better adapt to new data.

Transfer learning has several advantages. It leverages pre-trained models trained on large datasets, which can significantly reduce the time and resources needed to train a task-specific model. In addition, it makes it possible to improve the model's performance on limited data sets, by exploiting the general characteristics learned by the pre-driven model. However, transfer learning requires some similarity between the source task and the target task. The characteristics learned on the source task must be relevant and transferable to the target task. In addition, special attention should be paid to the selection of the pre-trained model, the management of differences in data distributions between tasks and the prevention of over-learning when adjusting the model.

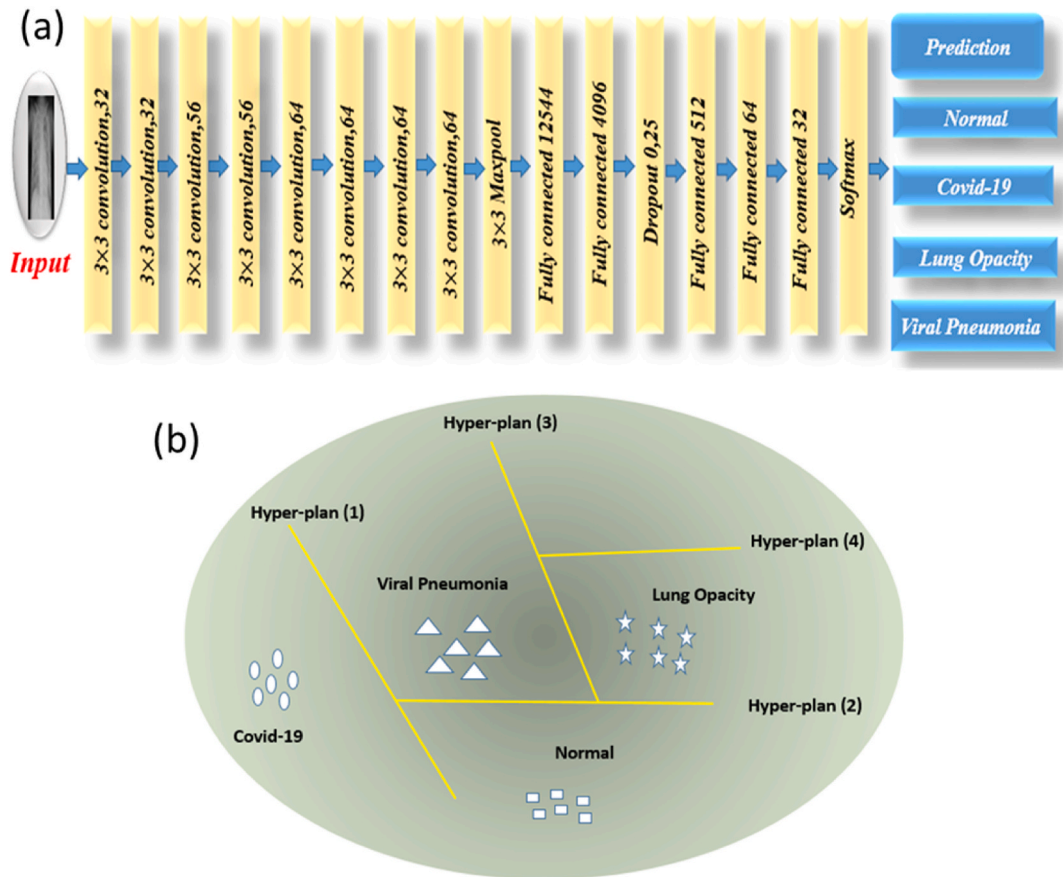In this study, three different transfer learning models were employed

Fig. 4. (a) The architecture of convolution neural network, (b) Classification with the support vector machine.
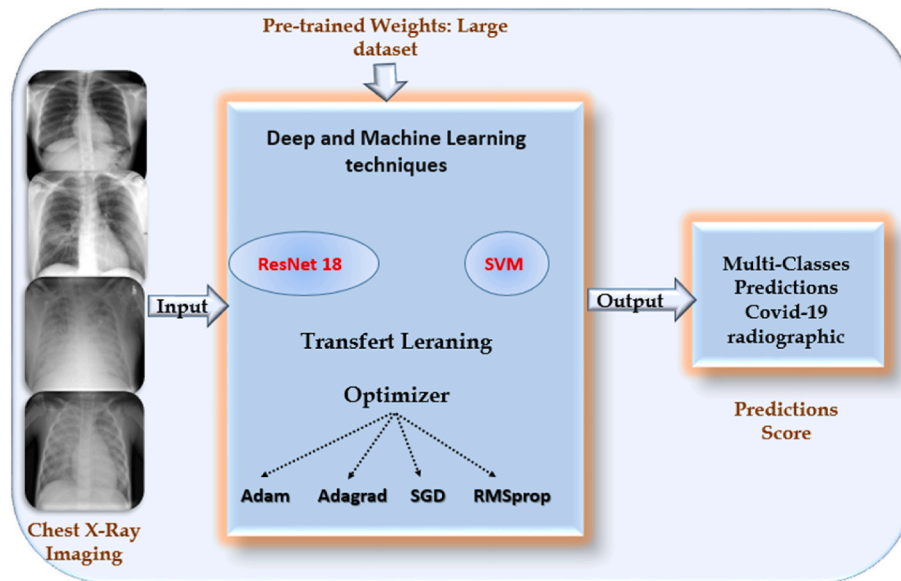

Fig. 5. Illustration of the transfer learning process of ResNet18-SVM model.

to evaluate their effectiveness on the task at hand: ResNet18-SVM, EfficientNet-CNN, and Xception-CNN. Each model was chosen for its specific strengths in feature extraction and task adaptability. Transfer learning is widely used in many areas, including computer vision, natural language processing and speech recognition. It has demonstrated its effectiveness in a variety of tasks, allowing researchers and practitioners to use previously acquired knowledge to solve new problems with greater precision and efficiency [36].

2.3. Model development

In the learning phase, and to reduce the error during each iteration, we adopt the Adam optimization algorithm [37]. The latter is an adaptive learning rate algorithm that has been designed specifically for

the formation of deep neural networks. Adam outperforms other optimization algorithms thanks to its advantage in relatively low memory requirements. Adam is an adaptive learning rate method that calculates individual learning rates based on various parameters. The adaptive learning rate adjustment involves modifying the learning rate during training, typically decreasing it according to a predetermined schedule. Similarly, the Adam algorithm combines the strengths of Stochastic Gradient Descent with Momentum (SGDM) and Root Mean Square Propagation (RMSProp). Unlike RMSProp, Adam incorporates a momentum term, which helps improve convergence [38]. This algorithm has two decay parameters that control the deformation rates of these calculated moving averages. The equations for ml, v_l, and θ_{l+1} in the parameter update for Adam are given as follows:

$$m_l = B_1 m_{l-1} + (1 - \beta_1) \nabla E(\theta_l) \tag{4}$$

$$v_l = B_2 v_{l-1} + (1 - \beta_2)\left[\nabla E(\theta_l)^2\right] \tag{5}$$

$$\theta_{l+1} = \theta_l - \frac{\alpha m_l}{\sqrt{v_l} + \varepsilon} \tag{6}$$

Where, m, $\nabla E(\theta)$, α, $\beta_1 (\beta_2)$ and v are the gradient moving averages, the loss function, learning rate θ, gradient decay factor (squared gradient decay factor), and squared gradient moving averages, respectively. l denotes the number of iterations. For each transfer learning model—ResNet18-SVM, EfficientNet-CNN, and Xception-CNN, the Adam optimizer was fine-tuned to ensure the best performance for the target dataset. Specific hyperparameters, such as learning rate and batch size, were adapted to suit the architecture and task requirements. This combination of adaptive learning rates and momentum ensures faster convergence and robust performance across various models and datasets.

3. Results and discussion

During the processing of medical data, it is necessary to reduce the number of false negatives as much as possible, especially in the case of infectious diseases such as COVID-19. The false negatives in diagnosing a patient with COVID-19 introduces not only inappropriate care and under-treatment, but of course incorrect medications that can affect the patient. Network classification performance was measured based on validation and test sets. Accuracy, precision, recall and F1-score were also investigated. In addition, the equations below demonstrate the calculation of metrics for each category of four classifications:

$$Accuracy = \frac{t_p + t_n}{t_p + f_p + t_n + f_n} \tag{7}$$

$$Precision = \frac{t_p}{t_p + f_p} \tag{8}$$

$$Recall = \frac{t_p}{t_p + f_n} \tag{9}$$

$$F1 - Score = \frac{2t_p}{2t_p + f_p + f_n} \tag{10}$$

With, t_p: refers to true positive classifications; f_n: represents false negative classifications; t_n: means true negative classifications, and finally f_p represents false positive classifications. In the medical context, researchers particularly rely on recall sensitivity to reduce false negatives. This sensitivity plays a crucial role in evaluating frameworks that distinguish patterns of COVID-19, normal conditions, viral pneumonia, and lung opacity, ensuring accurate representation within the specific population under consideration. Instead of solely relying on accuracy, which provides a general measure of classification performance, the F1-score offers a more reliable metric, particularly for imbalanced class distributions. Finally, to determine false negatives with desirable

accuracy, both recall and F1-score must be considered.

According to the multi-class classification of normal X-ray imaging, COVID-19, viral pneumonia and lung opacity, we classified the infected cases for the latter used deep learning, for which 3616 images of the COVID-19, 1345 images viral pneumonia cases, 6012 images lung opacity and 10192 normal patient images from the dataset. The initial dataset is divided into two sub-datasets, one for training and one for testing. In the split and train test, 80 % of the images were suitable for training and 20 % for testing. After the classification of the data set, the five models (CNN, VGG-16, VGG-19, ResNet-18 and SVM) were used for the exposed depth learning model. Figs. 6 and 7 represent the loss and accuracy curves.

As demonstrated by the accuracy and loss curves, we obtained the best results for the four models listed. For example, we find that the best epoch is 12 with an accuracy of 86 % and it drops to 83.49 % in the 19th epoch. The best epoch for VGG-16 is the 6th with 86 %, and it goes down to 75.35 %. For VGG-19, the second epoch is the best with 87 % and then it declines to 77.22 %. And for ResNet-18, the 19th epoch is the best with 86.18 % accuracy as plotted in Fig. 6. The training time for CNN on GPU was approximately 1.5 h, with a classification time of 5 min per batch. The same trend was observed for the VGG-16, VGG-19, and ResNet-18 models, with all of them trained efficiently on GPU. On the other hand, machine learning from SVM over-processed the X-ray data and resulted in an accuracy of 68 % in the validation set. The SVM model was trained using a CPU, and it took around 2 h for training, with a classification time of 15 min per batch. The performance comparison of these models in our study was conducted using the following metrics: accuracy, recall, precision, and F1 score, as presented in Table 2.

This study focused on diagnosing COVID-19 patients and differentiating them from non-COVID patients, lung opacity, and pneumonia based on X-ray images. X-ray imaging is a preferred medical imaging technique that is widely available in radiology centers and hospitals. In total, 21,156 images were used to train and test five developed models, which achieved excellent performance. From the analysis, we found that ResNet-18 is the best architecture for data classification due to its dual advantages: First, pre-processing is often unnecessary to test the viewed images, and the increased dataset size helps in resizing the test images. Then, the preformed CNN architecture is optimized using ADAM on X-ray images to avoid overfitting problems and to ensure optimal performance. ResNet-18, trained on GPU, showed a training time of approximately 1 h with a classification time of 10 min per batch. In contrast to this study, the cited studies encountered a notable limitation: while the dataset was optimized for diverse objectives and deep learning methodology yielded superior results, the computational load was substantial due to the utilization of a deep learning network (DL) aimed at enhancing efficiency. Optimal solutions must be well divided among all objectives to implement multi-objective optimization.

Similarly, in order to avoid over-learning of the model, regularization techniques such as dropout were used. The training was carried out over several periods until the model's performance reached satisfactory convergence. Thus, for the classification of radiographic images we used the SVM (Support Vector Machine) as a machine learning model. The characteristics extracted from the X-ray images using this model were used as inputs for the SVM which was evaluated by different kernel functions, such as the linear kernel, the Radial Basis Function (RBF) kernel and the polynomial kernel. We also compared the performance of different optimization functions, such as Stochastic Gradient Descent (SGD), Adam, Adagrad and RMSprop, etc., for the deep learning model and machine learning model. These were evaluated using measures such as accuracy, recall, F-measure and Precision. While deep learning models (CNN, VGG-16, VGG-19, and ResNet-18) provided faster classification times when trained on GPU, the SVM model, using CPU, required significantly more time for both training and classification.

Comparisons were also made between the different approaches to determine the most effective method for automatic detection of radiographic images in lung conditions. Deep learning models, trained on
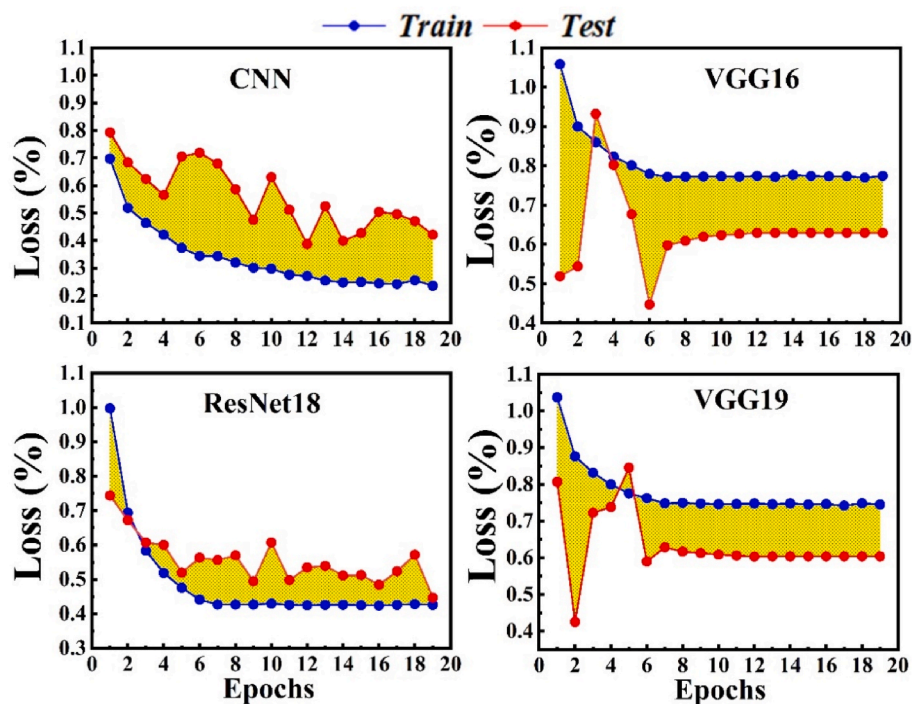
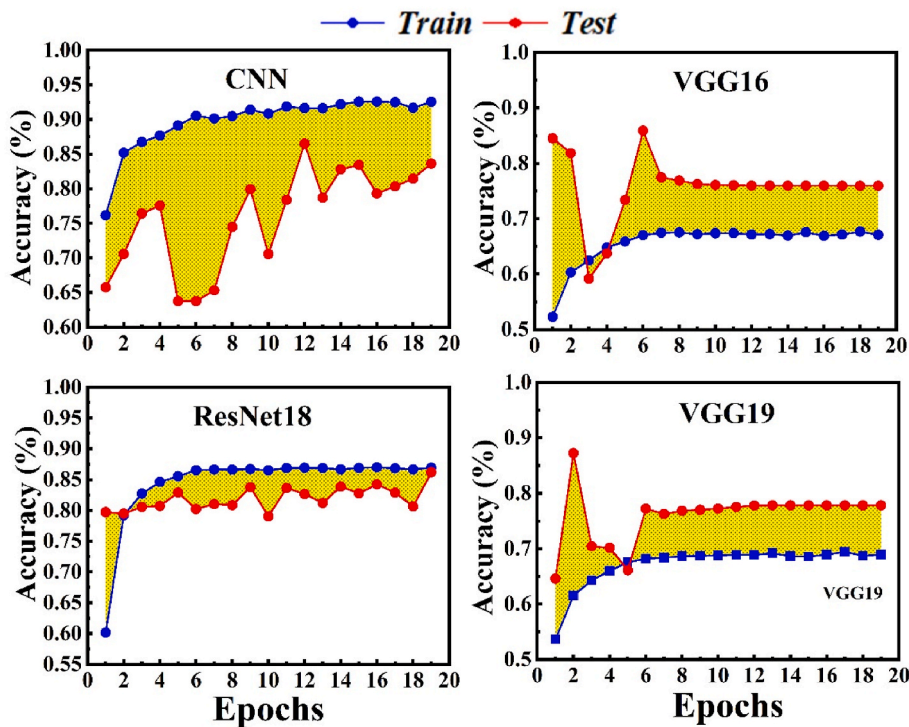**Fig. 6.** Loss curve of the models CNN, VGG-16, VGG-19, and ResNet-18.

Fig. 7. Accuracy curve of the models CNN, VGG-16, VGG-19, and ResNet-18.

GPU, outperformed traditional machine learning models like SVM in terms of training time and classification speed, while the SVM model's longer processing time may limit its practical use in real-time clinical settings. The ultimate goal of training a model is to minimize the loss function. Several classification parameters employed in this study are detailed in Table 3.

3.1. Comparison of different optimizers

In this investigation of transfer learning models for X-ray image recognition, we evaluated three architectures: ResNet18-SVM, EfficientNet-CNN, and Xception-CNN. Each model was trained using four optimizers: Adam, AdaGrad, SGD, and RMSProp. The results presented in Table 4 highlight the performance metrics, including accuracy, recall,

Table 2
Performance metrics for CNN, ResNet-18, VGG-16, VGG-19, and SVM models.

Architecture	Accuracy	Recall	Precision	F1-Mesure
CNN	0.834979	0.845421	0.826357	0.833452
ResNet-18	0.861866	0.835124	0.813381	0.857154
VGG-16	0.753590	0.732511	0.767412	0.743541
VGG-19	0.772297	0.786614	0.741284	0.773541
SVM	0.681534	0.672258	0.663585	0.692418

Table 3
Model parameter settings.

Initial weight	Image Net	Optimizer	Adam
Batch-size	64	Learn rate	$2\,e^{-5}$
Epoch	22	Loss	Categorical_CrossEntropyLoss

Table 4
Performance metrics for transfer learning models (ResNet18-SVM, EfficientNet-CNN, and Xception-CNN) with Adam, Adagrad, SGD, and RMSProp optimizers.

Metrics	Adam	Adagrad	SGD	RMSProp
ResNet18-SVM				
Accuracy	0.9704	0.9414	0.9848	0.9604
Recall	0.9673	0.9515	0.9718	0.9773
Precision	0.9858	0.9545	0.9648	0.9727
F1-Mesure	0.9885	0.9375	0.9747	0.9847
EffcientNet-CNN				
Accuracy	0.9920	0.9914	0.9919	0.9908
Recall	0.9875	0.9901	0.9810	0.9881
Precision	0.9848	0.9883	0.9902	0.9850
F1-Mesure	0.9887	0.9892	0.9886	0.9844
Xception-CNN				
Accuracy	0.9880	0.9856	0.9799	0.9832
Recall	0.9829	0.9811	0.9754	0.9777
Precision	0.9857	0.9842	0.9699	0.9816
F1-Mesure	0.9831	0.9830	0.9762	0.9793

precision, and F1-measure, for each model and optimizer combination.

The loss and accuracy curves for ResNet18-SVM (Fig. 8(a and b)) demonstrate that the model initially converges quickly after learning and then stabilizes. However, Adam's optimization technique provides faster convergence and better results.

For the EfficientNet-CNN model, the loss analysis and classification accuracy curves (Fig. 9(a and b)) indicate smoother and more stable convergence for Adam and RMSProp optimizers, while AdaGrad displayed the lowest convergence rate. Similarly, the loss variation and accuracy trends for Xception-CNN (Fig. 10(a and b)) highlight that Adam consistently outperformed other optimizers, achieving the highest performance metrics, whereas AdaGrad exhibited slower convergence and reduced accuracy.

The ResNet18-SVM model demonstrated strong performance across all optimizers. However, the AdaGrad optimizer exhibited the worst convergence, as evidenced by its relatively low accuracy and F1-measure scores. In contrast, Adam, SGD, and RMSProp provided significantly better convergence and performance. The loss and accuracy curves for ResNet18-SVM (Fig. 8) show that the model initially converges rapidly, stabilizing after several iterations. Among the optimizers, Adam stands out for its faster convergence and superior results, achieving the highest F1-measure of 0.9885. The accuracy plots for ResNet18-SVM (Fig. 8) highlight that AdaGrad converges poorly compared to the other optimizers. SGD demonstrates rapid convergence at the beginning of training but is surpassed by Adam in terms of stability and overall accuracy. This pattern is consistent across the other two models, EfficientNet-CNN and Xception-CNN, although with slight variations.

For the EfficientNet-CNN model, Adam consistently outperformed the other optimizers, achieving the highest accuracy (0.9920) and F1-measure (0.9887). AdaGrad and RMSProp showed competitive performance but slightly lagged behind Adam in terms of recall and precision. The loss curves and accuracy curves for EfficientNet-CNN (Fig. 9(a and b)) reveal smoother and more stable convergence compared to ResNet18-SVM, especially for Adam and RMSProp optimizers.

The Xception-CNN model displayed a similar trend, with Adam again leading in terms of performance metrics. Its accuracy reached 0.9880, and its F1-measure was 0.9831, slightly lower than EfficientNet-CNN but still indicative of strong performance. Interestingly, while SGD performed well for ResNet18-SVM, it showed reduced effectiveness for Xception-CNN, as evidenced by a lower F1-measure (0.9762). AdaGrad, as observed in the other models, exhibited the slowest convergence and the lowest accuracy (0.9856). The loss and accuracy curves for Xception-CNN (Fig. 10(a and b)) illustrate these observations across the four optimizers.

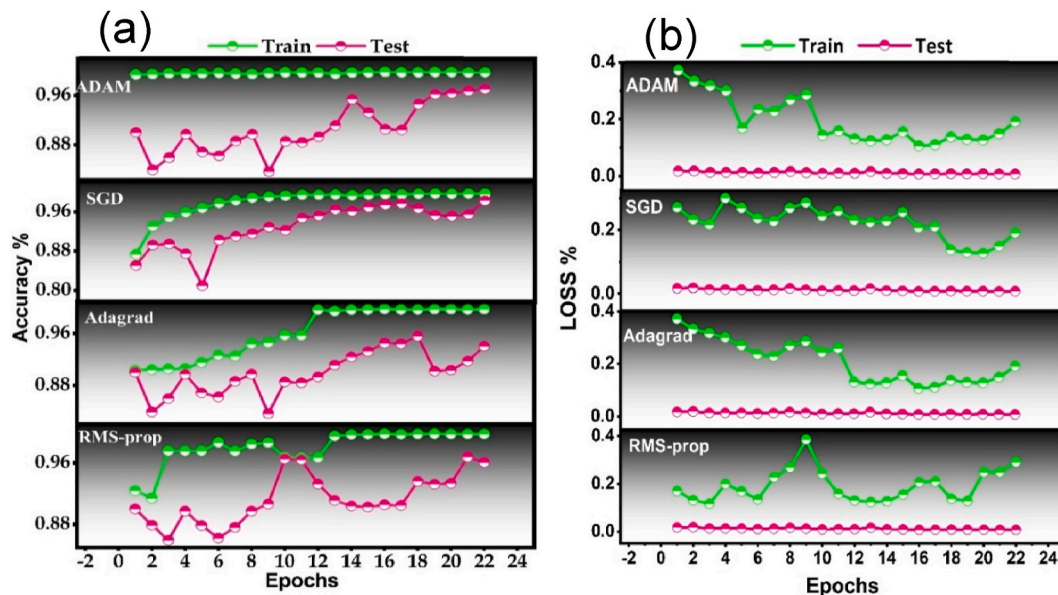In summary, Adam emerged as the most effective optimizer across all

Fig. 8. (a): Accuracy curve for the ResNet18-SVM model and (b): Loss curve for the ResNet18-SVM model.
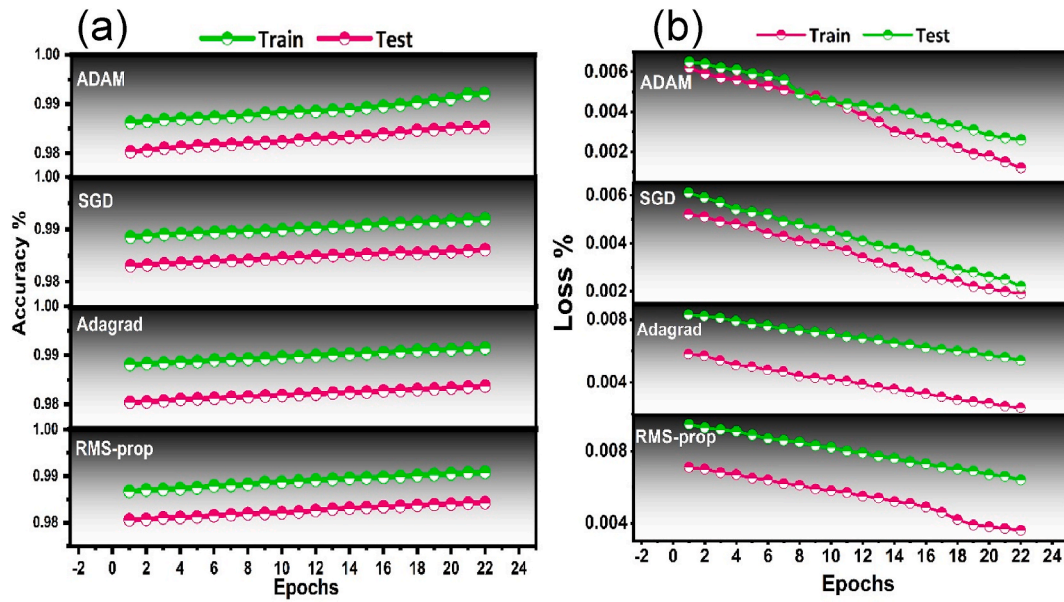
Fig. 9. (a): Accuracy analysis for the EfficientNet-CNN model and (b): Classification loss of the EfficientNet-CNN model.
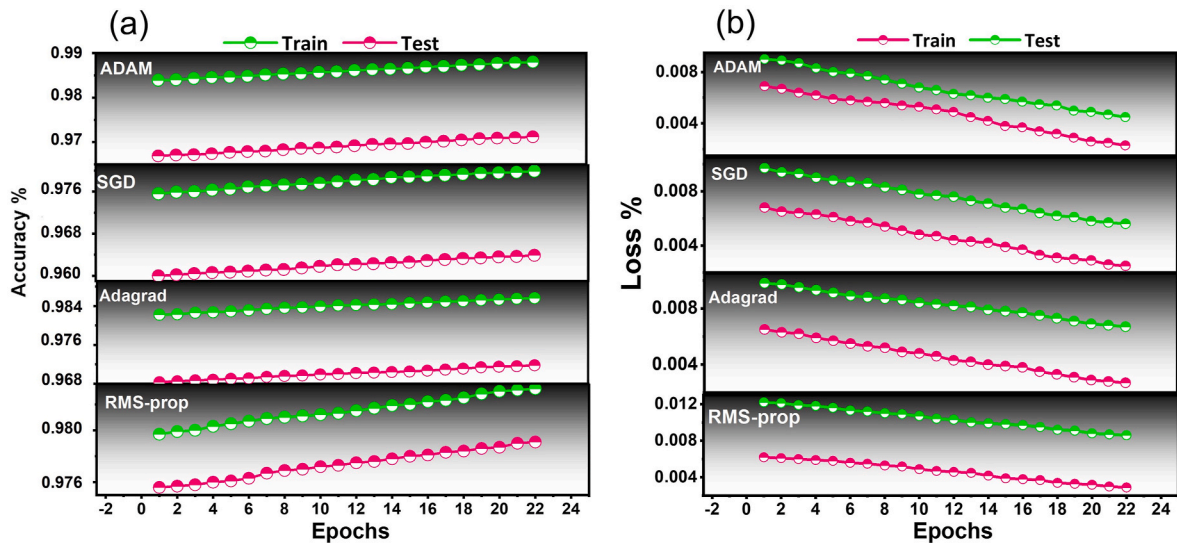

Fig. 10. (a): Accuracy variation for the Xception-CNN model and (b): Loss trends for the Xception-CNN model.

three models, consistently delivering the highest accuracy, precision, recall, and F1-measure scores. EfficientNet-CNN achieved the best overall performance among the three architectures, with Xception-CNN following closely. ResNet18-SVM, while effective, displayed greater variability across different optimizers.

To better understand the model training process, we monitored the loss and accuracy curves over the course of training. The loss curves demonstrate that Adam facilitates rapid and smooth convergence across all models, while AdaGrad suffers from slower convergence and occasional instability. The categorical cross-entropy loss function used in this study initially decreases significantly during training, eventually stabilizing near zero for the best-performing optimizers (Adam, RMSProp). EfficientNet-CNN's superior performance can be attributed to its ability to balance model complexity with efficient training, leveraging its unique architecture for feature extraction. Similarly, Xception-CNN's depthwise separable convolutions contribute to its high accuracy and stability, despite slightly lower precision compared to EfficientNet-CNN. ResNet18-SVM, while not as robust as the other two models, benefits

from its simplicity and computational efficiency, making it a viable option for specific tasks with limited resources.

3.2. Comparative analysis of several models

Numerous studies have examined the dataset in question, yet they have reported varying levels of accuracy. In three notable studies, the following results were documented: The first study categorized images into three classes—normal, pneumonia (including influenza-A viral pneumonia), and COVID-19—using CT lung images and deep learning, achieving an overall accuracy of 86 % [6]. The second study, which focused on four classes (normal, COVID-19, macro average, and weighted average), employed a CNN for classification and reported an accuracy of 85 % [39]. The third study used VGG-19 to classify images into three classes (normal, pneumonia, and COVID-19), attaining an accuracy of 83 % [7]. In contrast, our study outperforms these previous works by utilizing four classes and achieving an accuracy of 86.18 % with the ResNet-18 architecture. This indicates the effectiveness of our

approach in categorizing radiographic images more comprehensively. We selected the most advanced deep learning models available for image classification to rigorously evaluate the effectiveness of our proposed models.

Further comparative analyses have been conducted on images derived from CT scans. One study focused on binary classification (normal vs. COVID-19) and achieved an impressive overall accuracy of 97 %. Another study, aiming for automated pneumonia detection in COVID-19 diagnoses, utilized a fitted ResNet model that resulted in an overall accuracy of 95.65 %, with 92.74 % specificity and 95.90 % sensitivity [40]. A third study also concentrated on binary classification between normal and COVID-19, employing methodologies developed with 746 tomodensitometric images. This study reported F1 scores of 0.98 for sensitivity, specificity, accuracy, and precision [41]. To further enhance our model's performance, we recommend exploring comparative studies with advanced techniques such as attention mechanisms (e. g., spatial and temporal attention, attention pyramid networks) and deformable convolution. Relevant articles for this exploration include.

- "A triple interference removal network based on temporal and spatial attention interaction for forest smoke recognition in videos."
- "Smoke recognition in satellite imagery via an attention pyramid network with bidirectional multi-level multi-granularity feature aggregation and gated fusion."
- "A label-relevance multi-direction interaction network with enhanced deformable convolution for forest smoke recognition."

Table 5 summarizes the results of these comparative studies, highlighting the potential improvements that could be achieved by integrating more sophisticated methodologies.

4. Conclusion

In conclusion, we developed and evaluated deep learning methods and transfer learning approaches to enhance the detection and classification of COVID-19 and other pulmonary conditions using radiographic

Table 5
Comparison of COVID-19 detection studies using CT images across various models and classes.

STUDY	Classes	Used model	Accuracy	Ref
1	Normal, COVID-19, lung opacity, and viral pneumonia	CNN	83.49 %	This work
		ResNet-18	86.18 %	
		VGG-16	75.35 %	
		VGG-19	77.22 %	
		SVM	68.15 %	
2	Normal, pneumonia (IAVP), COVID-19.	Deep learning	86 %	[6]
3	Normal, COVID-19, Macro average, Weithed average.	CNN	85 %	[39]
	Normal, pneumonia, COVID-19.	VGG-19	83 %	[7]
4	Normal, COVID-19, lung opacification, viral pneumonia.	ResNet-19	86.18 %	
	Normal, COVID-19	Deep Learning	97 %	
5	Normal, COVID-19	ResNet	95 % accuracy, 95.65 % sensitivity, 92.74 % specificity, 95.9 % precision	[40]
6	Normal, COVID-19	Classifier based on test sample	F1: 0.98, Accuracy: 0.98, Sensitivity: 0.98, Specificity: 0.97	[41]
7	COVID-19 Non-COVID	DenseNet201	98.73 % 91.67 %	[18]
		ResNet152	97.23 % 89.45 %	
		VGG16	91.25 % 85.34 %	
		InceptionV3	98.38 % 92.33 %	

images. Our first study focused on utilizing convolutional neural networks (CNN) and their architectures—VGG-16, VGG-19, and ResNet-18—alongside SVM machine learning to identify COVID-19, achieving accuracies of 83 % for CNN, 75 % for VGG-16, 77 % for VGG-19, 86 % for ResNet-18, and 68 % for SVM. These results demonstrate that CNN architectures, particularly ResNet-18, are effective for COVID-19 detection. This method aims to enhance medical capabilities in areas with limited radiotherapy resources, facilitating early identification of COVID-19 to prevent severe consequences such as death. Despite these promising results, our method has limitations, including variable accuracies across models and the presence of false negatives and positives. These limitations highlight the need for further improvements in the models for greater robustness and reliability. Our research provides valuable insights for researchers and practitioners in the fields of pattern recognition and medical imaging. The proposed methods can be adapted and extended to other medical domains requiring precise image classification, thus contributing to the improvement of medical diagnostics and patient care. In our second study, we employed transfer learning with a ResNet18-SVM model for multiclass classification of radiographic images. This model, pre-trained on the ImageNet dataset, was optimized with various algorithms such as Adam, AdaGrad, SGD, and RMSProp, achieving classification rates of 98 % for SGD, 97 % for Adam, 96 % for RMSProp, and 94 % for AdaGrad, outperforming traditional methods. Additionally, we explored two other transfer learning models, EfficientNet-CNN and Xception-CNN, which also demonstrated impressive performance with accuracies of 99.20 % for EfficientNet-CNN and 98.80 % for Xception-CNN. These results further validate the effectiveness of transfer learning in improving classification performance for radiographic image recognition.

Future work will focus on several areas: exploring hybrid features to improve accuracy by reducing false negatives and positives; enhancing the completeness and representativeness of radiographic image data to cover a greater diversity of clinical cases; developing specialized recognition algorithms to further advance medical image recognition capabilities; and conducting clinical studies to evaluate the effectiveness and acceptability of the proposed methods in real-world settings. These combined efforts underscore the importance of leveraging advanced machine learning techniques to improve the accuracy and efficiency of medical diagnoses, particularly in the context of limited resources and critical health emergencies. By working on these fronts, we hope to significantly contribute to the enhancement of diagnostic and treatment capabilities for pulmonary conditions worldwide.

CRediT authorship contribution statement

Hajar Lamouadene: Methodology, Investigation, Formal analysis. **Majid EL Kassaoui:** Validation, Methodology, Investigation. **Mourad El Yadari:** Resources, Methodology. **Abdallah El Kenz:** Investigation, Formal analysis, Conceptualization. **Abdelilah Benyoussef:** Validation, Supervision, Methodology. **Amine El Moutaouakil:** Writing – review & editing, Writing – original draft, Supervision, Project administration, Conceptualization. **Omar Mounkachi:** Supervision, Project administration, Conceptualization.

Ethics statement

The research conducted in the paper titled: "Detection of COVID-19, Lung Opacity, and Viral Pneumonia via X-ray Using Machine Learning and Deep Learning" does not need any ethics statement, since that all the used X-ray data has been downloaded from the Kaggle database at https://www.kaggle.com/tawsifurrahman/covid19-radiography-database.

Declaration of competing interest

The authors declare that they have no known competing financial interests or personal relationships that could have appeared to influence

the work reported in this paper.

References

[1] S. Zhao, Z. Li, Y. Chen, W. Zhao, X. Xie, J. Liu, D. Zhao, Y. Li, SCOAT-net: a novel network for segmenting COVID-19 lung opacification from CT images, Pattern Recogn. 119 (2021) 108109, https://doi.org/10.1016/j.patcog.2021.108109.

[2] S. Asif, Y. Wenhui, S.- ur-Rehman, Q.- ul-ain, K. Amjad, Y. Yueyang, S. Jinhai, M. Awais, Advancements and prospects of machine learning in medical diagnostics: unveiling the future of diagnostic precision, Arch Computat Methods Eng (2024), https://doi.org/10.1007/s11831-024-10148-w.

[3] S.S. Chong, Y.S. Ng, H.-Q. Wang, J.-C. Zheng, Advances of machine learning in materials science: ideas and techniques, Front. Phys. 19 (2023) 13501, https://doi.org/10.1007/s11467-023-1325-z.

[4] H. Lamouadene, M.E. Kassaoui, M. El Yadari, A. El Kenz, A. Benyoussef, Exploring modeling techniques for predicting band gaps of doped-ZnO: a machine learning approach, Chem. Phys. (2025) 112603.

[5] D. Zhao, Y. Liu, H. Yin, Z. Wang, An attentive and adaptive 3D CNN for automatic pulmonary nodule detection in CT image, Expert Syst. Appl. 211 (2023) 118672, https://doi.org/10.1016/j.eswa.2022.118672.

[6] X. Xu, X. Jiang, C. Ma, P. Du, X. Li, S. Lv, L. Yu, Q. Ni, Y. Chen, J. Su, et al., A deep learning system to screen novel coronavirus disease 2019 pneumonia, Engineering 6 (2020) 1122–1129, https://doi.org/10.1016/j.eng.2020.04.010.

[7] M.J. Horry, S. Chakraborty, M. Paul, A. Ulhaq, B. Pradhan, M. Saha, N. Shukla, X-Ray Image Based COVID-19 Detection Using Pre-trained Deep Learning Models, 2020.

[8] E. Waisberg, J. Ong, S.A. Kamran, P. Paladugu, N. Zaman, A.G. Lee, A. Tavakkoli, Transfer learning as an AI-based solution to address limited datasets in space medicine, Life Sci. Space Res. 36 (2023) 36–38, https://doi.org/10.1016/j.lssr.2022.12.002.

[9] X. Li, H. Jiang, X. Xiong, H. Shao, Rolling bearing health prognosis using a modified health index based hierarchical gated recurrent unit network, Mech. Mach. Theor. 133 (2019) 229–249, https://doi.org/10.1016/j.mechmachtheory.2018.11.005.

[10] S. Haidong, C. Junsheng, J. Hongkai, Y. Yu, W. Zhantao, Enhanced deep gated recurrent unit and complex wavelet packet energy moment entropy for early fault prognosis of bearing, Knowl. Base Syst. 188 (2020) 105022, https://doi.org/10.1016/j.knosys.2019.105022.

[11] Highly accurate machine fault diagnosis using deep transfer learning, Available online: https://ieeexplore.ieee.org/document/8432110/?denied=. (Accessed 16 October 2023).

[12] F. Jia, Y. Lei, N. Lu, S. Xing, Deep normalized convolutional neural network for imbalanced fault classification of machinery and its understanding via visualization, Mech. Syst. Signal Process. 110 (2018) 349–367, https://doi.org/10.1016/j.ymssp.2018.03.025.

[13] C. Xu, B.T. Cao, Y. Yuan, G. Meschke, Transfer learning based physics-informed neural networks for solving inverse problems in engineering structures under different loading scenarios, Comput. Methods Appl. Mech. Eng. 405 (2023) 115852, https://doi.org/10.1016/j.cma.2022.115852.

[14] Classification and Mutation Prediction from Non–Small Cell Lung Cancer Histopathology Images Using Deep Learning | Nat. Med. Available online: https://www.nature.com/articles/s41591-018-0177-5 (accessed on 17 October 2023)..

[15] High-Throughput Adaptive Sampling for Whole-Slide Histopathology Image Analysis (HASHI) via Convolutional Neural Networks: Application to Invasive Breast Cancer Detection | PLoS One Available online: https://journals.plos.org/plosone/article?id=10.1371/journal.pone.0196828 (accessed on 17 October 2023)..

[16] Q. Zheng, L. Yang, B. Zeng, J. Li, K. Guo, Y. Liang, G. Liao, Artificial intelligence performance in detecting tumor metastasis from medical radiology imaging: a systematic review and meta-analysis, eClinicalMedicine 31 (2021), https://doi.org/10.1016/j.eclinm.2020.100669.

[17] M.C.A. Balkenhol, D. Tellez, W. Vreuls, P.C. Clahsen, H. Pinckaers, F. Ciompi, P. Bult, J.A.W.M. van der Laak, Deep learning assisted mitotic counting for breast cancer, Lab. Invest. 99 (2019) 1596–1606, https://doi.org/10.1038/s41374-019-0275-0.

[18] V. Chang, S. Mcwann, K. Hall, Q.A. Xu, M.A. Ganatra, Diagnosis of COVID-19 CT scans using convolutional neural networks, SN COMPUT. SCI. 5 (2024) 625, https://doi.org/10.1007/s42979-024-02878-2.

[19] Automated brain histology classification using machine learning - ScienceDirect, Available online: https://www.sciencedirect.com/science/article/pii/S0967586819306563. (Accessed 17 October 2023).

[20] Systematic Review of Machine Learning for Diagnosis and Prognosis in Dermatology: J. Dermatol. Treat.: Vol 31, No 5 Available online: https://www.tandfonline.com/doi/abs/10.1080/09546634.2019.1682500 (accessed on 17 October 2023)..

[21] Predicting Non-Small Cell Lung Cancer Prognosis by Fully Automated Microscopic Pathology Image Features | Nat. Commun. Available online: https://www.nature.com/articles/ncomms12474 (accessed on 17 October 2023)..

[22] X. Luo, X. Zang, L. Yang, J. Huang, F. Liang, J. Rodriguez-Canales, I.I. Wistuba, A. Gazdar, Y. Xie, G. Xiao, Comprehensive computational pathological image analysis predicts lung cancer prognosis, J. Thorac. Oncol. 12 (2017) 501–509, https://doi.org/10.1016/j.jtho.2016.10.017.

[23] Pathologist-Level Classification of Histologic Patterns on Resected Lung Adenocarcinoma Slides with Deep Neural Networks | Sci. Rep. Available online: https://www.nature.com/articles/s41598-019-40041-7 (accessed on 17 October 2023)..

[24] Diagnostics | free full-text | an efficient deep learning method for detection of COVID-19 infection using chest X-ray images, Available online: https://www.mdpi.com/2075-4418/13/1/131. (Accessed 27 August 2023).

[25] A. Mikołajczyk, M. Grochowski, Data augmentation for improving deep learning in image classification problem, in: Proceedings of the 2018 International Interdisciplinary PhD Workshop, IIPhDW), May 2018, pp. 117–122.

[26] G. Dhiman, V. Chang, K. Kant Singh, A. Shankar, ADOPT: automatic deep learning and optimization-based approach for detection of novel coronavirus COVID-19 disease using X-ray images, J. Biomol. Struct. Dyn. 40 (2022) 5836–5847, https://doi.org/10.1080/07391102.2021.1875049.

[27] A.M. Elmoogy, X. Dong, T. Lu, R. Westendorp, K.R. Tarimala, SurfCNN: a descriptor accelerated convolutional neural network for image-based indoor localization, IEEE Access 8 (2020) 59750–59759, https://doi.org/10.1109/ACCESS.2020.2981620.

[28] K. He, X. Zhang, S. Ren, J. Sun, Deep Residual Learning for Image Recognition, 2016, pp. 770–778.

[29] W. Chen, H.R. Pourghasemi, A. Kornejady, N. Zhang, Landslide spatial modeling: introducing new ensembles of ANN, MaxEnt, and SVM machine learning techniques, Geoderma 305 (2017) 314–327, https://doi.org/10.1016/j.geoderma.2017.06.020.

[30] N. Cristianini, B. Scholkopf, Support vector machines and kernel methods: the new generation of learning machines, AI Mag. 23 (2002), https://doi.org/10.1609/aimag.v23i3.1655, 31–31.

[31] M. Marjanović, M. Kovačević, B. Bajat, V. Voženílek, Landslide susceptibility assessment using SVM machine learning algorithm, Eng. Geol. 123 (2011) 225–234, https://doi.org/10.1016/j.enggeo.2011.09.006.

[32] X. Yao, L.G. Tham, F.C. Dai, Landslide susceptibility mapping based on support vector machine: a case study on natural slopes of Hong Kong, China, Geomorphology 101 (2008) 572–582, https://doi.org/10.1016/j.geomorph.2008.02.011.

[33] A. Statnikov, C.F. Aliferis, D.P. Hardin, I. Guyon, Gentle Introduction to Support Vector Machines in Biomedicine, A - Volume 2: Case Studies and Benchmarks, World Scientific Publishing Company, 2013, 978-981-4518-50-5.

[34] A novel image-based transfer learning framework for cross-domain HVAC fault diagnosis: from multi-source data integration to knowledge sharing strategies - ScienceDirect, Available online: https://www.sciencedirect.com/science/article/pii/S0378778822001669. (Accessed 17 October 2023).

[35] W. Yang, Y. Xie, A. Lin, X. Li, L. Tan, K. Xiong, M. Li, J. Lin, End-to-End open-domain question answering with BERTserini, in: Proceedings of the Proceedings of the 2019 Conference of the, North, 2019, pp. 72–77.

[36] A deep neural network-based method for deep information extraction using transfer learning strategies to support automated compliance checking - ScienceDirect, Available online: https://www.sciencedirect.com/science/article/pii/S0926580521002855. (Accessed 17 October 2023).

[37] Application of deep learning in neuroradiology: brain haemorrhage classification using transfer learning, Available online: https://www.hindawi.com/journals/cin/2019/4629859/. (Accessed 27 August 2023).

[38] M.N.Y. Ali, M.G. Sarowar, M.L. Rahman, J. Chaki, N. Dey, J.M.R.S. Tavares, Adam deep learning with SOM for human sentiment classification, Int. J. Ambient Comput. Intell. (IJACI) 10 (2019) 92–116, https://doi.org/10.4018/IJACI.2019070106.

[39] A. Waheed, M. Goyal, D. Gupta, A. Khanna, F. Al-Turjman, P.R. Pinheiro, CovidGAN: data augmentation using auxiliary classifier gan for improved covid-19 detection, IEEE Access 8 (2020) 91916–91923, https://doi.org/10.1109/ACCESS.2020.2994762.

[40] D. Arias-Garzón, J.A. Alzate-Grisales, S. Orozco-Arias, H.B. Arteaga-Arteaga, M.A. Bravo-Ortiz, A. Mora-Rubio, J.M. Saborit-Torres, J.Á.M. Serrano, M. de la Iglesia Vayá, O. Cardona-Morales, et al., COVID-19 detection in X-ray images using convolutional neural networks, Machine Learning with Applications 6 (2021) 100138, https://doi.org/10.1016/j.mlwa.2021.100138.

[41] S. Pathan, P.C. Siddalingaswamy, P. Kumar, M.M.M. Pai, T. Ali, U.R. Acharya, Novel ensemble of optimized CNN and dynamic selection techniques for accurate covid-19 screening using chest CT images, Comput. Biol. Med. 137 (2021) 104835, https://doi.org/10.1016/j.compbiomed.2021.104835.